Insights into hierarchically meso–macroporous structured materials†

Zhong-Yong Yuan and Bao-Lian Su*

Received 30th August 2005, Accepted 10th October 2005
First published as an Advance Article on the web 17th November 2005
DOI: 10.1039/b512304f

A great deal of progress has recently been made in the field of ordered porous materials having uniform channel dimensions which can be adjusted over a wide range of length scales. Incorporation of macropores in mesoporous materials combines benefits from both the mesoporous and macroporous structures. Hierarchical materials containing both interconnected macroporous and mesoporous structures have enhanced properties compared with single-sized pore materials due to increased mass transport through the material and maintainance of a specific surface area on the level of fine pore systems. Bimodal mesoporous–macroporous inorganic materials can be prepared by using a self-assembling surfactant or amphiphilic block copolymer species in conjunction with macrotemplates such as colloidal crystals, polymer foams, bio-celluloses, emulsions, inorganic salts and ice crystals, or by macroscopic phase separations. Here, we review the state of the art for hierarchical meso–macroporous inorganic materials and their carbon replicas from the viewpoint of synthesis strategies and emerging applications. Detailed synthetic processes are described, in which the very recently developed spontaneous formation of meso–macroporous (single and binary) metal oxides, metal phosphates and aluminosilicates is specifically addressed. These novel meso–macroporous materials have found a number of applications, including HPLC separation, catalysis, fuel cell electrode materials, biomaterials engineering, controlled drug delivery devices, and membrane reactors, and these are discussed illustratively.

Laboratory of Inorganic Materials Chemistry, The University of Namur (FUNDP), 61 rue de Bruxelles, B-5000 Namur, Belgium. E-mail: bao-lian.su@fundp.ac.be; Fax: +32-81-725414; Tel: +32-81-4531
† Presented at Symposium T: Porous materials for emerging applications, International Conference on Materials for Advanced Technologies (ICMAT 2005), Singapore, 3–8 July 2005

1 Introduction

Porous materials continue to attract great research interest and have made a great impact in many applications, including catalysis, sorption, and separation.[1] Based on a single molecular or ionic template or the assembly of organic templates, microporous (pore size below 2 nm), mesoporous (2–50 nm)

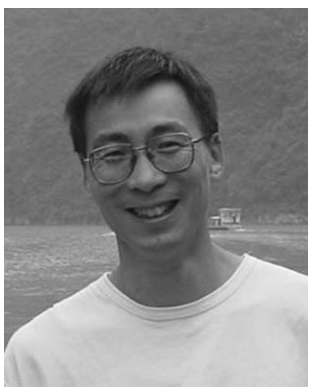

Zhong-Yong Yuan

Zhong-Yong Yuan was born in China in 1968. He received his BSc degree in chemistry at Zhejiang Normal University in 1990, and obtained his MSc and PhD degrees in physical chemistry at Nankai University in 1996 and 1999 respectively. After this he did postdoctoral research at the Beijing Laboratory of Electron Microscopy, Institute of Physics, Chinese Academy of Sciences. In 2001, he joined the Laboratory of Inorganic Materials Chemistry (CMI) at the University of Namur, Belgium. In 2006, he will become a Professor in the College of Chemistry at Nankai University, China. His current research is focused on the self-assembly of hierarchically nanoporous and nanostructured materials for applications in heterogeneous catalysis, sensor and electrode materials.

Bao-Lian Su

Bao-Lian Su received his BSc from the University of Liaoning in 1983, and MSc from the Chengdu Institute of Organic Chemistry, Chinese Academy of Sciences in 1986. He obtained his PhD in 1992 at the Université Pierre et Marie Curie. This was followed by postdoctoral research in the Laboratory of Catalysis at the University of Namur, Belgium in 1993–1994. After holding a research position at Catalytica Inc. (Mountain View, California), in September, 1995 he joined the faculty at the University of Namur and founded the Laboratory of Inorganic Materials Chemistry (CMI). He is currently a Full Professor of Inorganic and Materials Chemistry and the Director of the Laboratory of Inorganic Materials Chemistry. Prof. Su has received a series of honours and awards and published 150 scientific papers and three patents. His current research fields include the synthesis, properties and molecular engineering of organized and hierarchically porous materials and nanostructures for nanotechnology, biotechnology, information technology and biomedical applications.

and macroporous (exceeding 50 nm) solids can be produced efficiently.[2] Surfactants and amphiphilic copolymers can be used as templates to synthesize ordered mesoporous materials,[3,4] and periodic three-dimensional arrays of macropores have been fabricated using latex spheres as templates.[5] Many efforts have been devoted to the synthesis, characterization and applications of uniform mesoporous materials over the last decade, due to their attractive textual and structural features, *e.g.* highly ordered structures, ultrahigh surface areas and narrow pore size distributions in the mesopore range, tuneable pore size and pore structure. Progress has been made in structural, compositional, and morphological control and the stability of mesoporous materials for their emerging applications in catalysis, adsorption, sensors, and biotechnologies. The demand for applications in the encapsulation and separation of proteins, where biomolecules with large molecular weights are involved, drove the development of ordered mesoporous silicas with very large pore sizes, near 30 nm.[4,6]

Practical applications require mesoporous materials having hierarchical pore structures at different length scales in order to achieve highly organized functions, since the limited diffusibility of substrates through confined nano-channels can be a problem. The introduction of secondary larger pores has been demonstrated to improve remarkably the activity of mesoporous catalysts due to the enhanced diffusion of reactants and products.[7] Bimodal mesoporous silicas having small and large mesopores have been reported.[8–13] Post-treatment of hexagonal mesoporous silica in ammonia solution results in the formation of bimodal mesoporous silicas having interconnected pore systems.[8] Non-ionic, alkyl PEO surfactant templated [Si]-MSU-X mesoporous silicas having two kinds of mesopores in the pore size range 3–9 nm were prepared by adding sodium salt electrolyte solutions to the mixture gel.[9] Sun *et al.*[11] presented a method of cross-linking the primary mesoporous ($\sim$3 nm) materials with a triblock copolymer to form a material with a secondary pore distribution around 20 nm. However, all of these secondary larger mesopores are disordered. Moreover, these reported methods are difficult to apply to the preparation of bimodal mesoporous metal oxides.

The incorporation of ordered macropores in mesoporous materials may be somewhat more interesting and useful for catalysis and for engineering pore systems, in comparison to bimodal mesopore size distributions. From the viewpoint of applications, for instance in catalysis, the active sites are often located in the micropores and mesopores, while the macropores favour mass transfer and reduce transport limitations. This becomes particularly important for large molecules (*e.g.*, polymers, biomolecules) or in viscous systems, where diffusion rates are low. For the sake of large performance improvement, such materials should possess adjustable and well-defined macropores and tuneable, interconnected mesopore types of different size in the macropore walls. On all length scales, the larger pores should be connected *via* smaller pores. Thus, it remains a challenge to fabricate hierarchically bimodal mesoporous–macroporous materials with controlled individual pore sizes and pore structures, although several methods have been reported which combine the individual technologies of mesopore and macropore synthesis, for example, by dual templating of surfactants and colloid crystals.[14]

In this article, we address and critically review the state of the art research for the synthesis of hierarchically mesoporous–macroporous structured materials. The detailed synthesis strategies of bimodal (or multimodal) meso–macroporous materials with flexible compositions and pore structures are outlined. The emerging applications of these innovative, multi-scaled porous materials are discussed. This article will not, however, address the hierarchically bimodal micro–mesoporous[15,16] or micro–macroporous[17–19] materials that could be prepared using microporous zeolitic colloids as nanoparticle building blocks with the combination of supermolcular assembly or macrotemplating respectively.

2 The synthesis strategies of hierarchical oxides

In the synthesis of hierarchical mesoporous–macroporous inorganic oxide-based materials, self-assembled molecular aggregates or supramolecular assemblies are generally employed as the structure-directing agents of mesostructures. Meanwhile, some large-sized substances, such as colloidal crystals, polymer foams, bio-celluloses, emulsions, vesicles, inorganic salt and ice crystals, are added in the synthesis to direct the creation of macroporous structures. Careful control of the phase separation in the synthesis gel can also be applied to fabricate the hierarchical porous structures. In this section, a detailed description of the synthesis strategies of hierarchical meso–macroporous oxides is provided.

2.1 Colloidal crystals as macrotemplates with combination of supramolecular templating

The combination of surfactant and colloidal crystal templating methods offers an efficient way for the construction of ordered and interconnected mesoporous–macroporous architectures.[14,19–21] Colloids are usually considered as small particles with at least one characteristic dimension in the range of a few tens of nanometres to one micrometre. Colloidal latex spheres, all having the same diameter, are allowed to aggregate in a regular fashion, then the inorganic precursors and surfactant (or copolymer) micellar solution is allowed to infiltrate the spaces between the spheres, and this is followed by condensation and crystallization. The removal of the surfactant and latex spheres, by either high-temperature calcination or solvent extraction, leads to the formation of three-dimensional (3D) ordered meso–macroporous materials (Fig. 1).[14] The macroporous walls are composed of mesopores, and both pore types are interconnected. Such hierarchical materials of various compositions, including titania,[14] silica,[14,20,22,23] niobia,[14] and silica–alumina,[24] have been reported, and the multiple-scale structural organization formed makes it possible to tune the physical properties of the materials over a wide range of chemical compositions. Furthermore, by using two diameter-sized colloidal crystals, dual 3D macroporous silica structures can be synthesized. Luo *et al.*[23] synthesized 3D cubic ordered macroporous (140 nm) and binary macroporous (140, 80 nm) silica structures with ordered mesoporous (7.7 nm) walls by using cubic closed-packing equal-sized or binary-sized polystyrene (PS) spheres as templates respectively, and the triblock copolymer P123 as a mesostructure-directing agent.

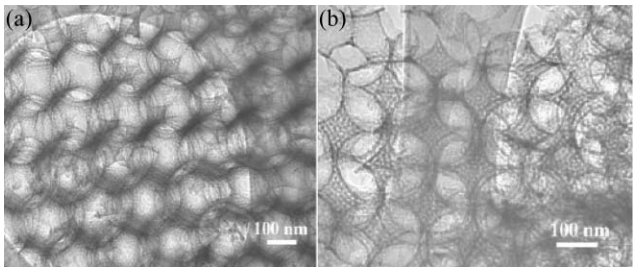

Fig. 1 TEM images of hierarchical silicas, showing that the framework of the macroporous skeleton is made up of ordered mesoporous silica.[14]

A silicate having a bimodal meso–macropore size distribution can be made by the sedimentation–aggregation technique,[25] in which the gel for the synthesis of a mesophase is generated by self-assembly of the surfactant and the silica precursor infiltrates the voids of the agglomerated PS particles. Random packing of latex beads covered with silica occurred after the addition of latex spheres to a mixed solution containing both cetyltrimethylammonium chloride/hydroxide and tetraethylorthosilicate, resulting in an eggshell type macrostructure morphology with an MCM-48-type cubic mesophase.[26] It has also been demonstrated that mixing latex beads with surfactant micellar solution before adding the inorganic source could produce a relatively uniform dispersion of macropores in the mesoporous MCM-48 materials.[26] Using this method, skeletal-structured biporous silicates with both a MCM-41 mesophase and a skeletal macrophase having an ordered array are reported, formed *via* microcolloidal crystal templating (Fig. 2).[27] The synthesized macrostructured MCM-41 (MS-MCM-41), obtained after impregnation of latex spheres at a controlling step and calcination of the polymer and surfactant, showed a superior 3D ordered macroporous structure extending from several, to hundreds of micrometres. The mesoporous phase located between the walls of the macropores contained the same structure as MCM-41, having a BET surface area above 1200 $m^2\ g^{-1}$, with a pore volume of about 1.27 $cm^3\ g^{-1}$. The specific volume of MS-MCM-41, accounting for both meso- and macropores,

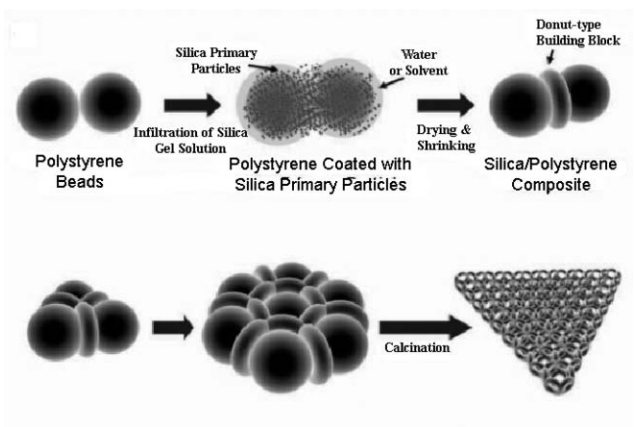

Fig. 2 A plausible schematic mechanism for the formation of skeletal-macrostructured MCM-41.[27]

was estimated to be 7.9 $cm^3\ g^{-1}$, using a simple density measurement. Fig. 2 proposes a plausible mechanism for the formation of skeletal macrostructures. The PS beads are coated with silicate primary particles, and then the doughnut-type building blocks are formed in the interstices of adjacent PS spheres through the drying and shrinking of the silica-precursor solution. These building units are expanded and arranged into the face-centered cubic (fcc) close-packed PS bead particles, and the skeletal structure of MS-MCM-41 is obtained after calcination of PS spheres. The inner space of the doughnut-type building block might make the interconnecting channels between macropores.

The advantage of this method, despite template sacrifice, is that organic functional molecules, such as a dye, can be directly incorporated into the framework of meso–macroporous materials. For example, mesostructured silica functionalized with the dye moiety, (2,4-dinitrophenylamine), has been prepared with control of the hierarchical pore architecture.[21] Co-condensation of tetraethoxysilane and 3-(2,4-dinitrophenylamino)propyltriethoxysilane was used to covalently couple the organic chromophore to the wall structure of a silica mesophase formed by surfactant templating of cetyltrimethylammonium bromide (CTAB). This process was spatially patterned at the macroscale by confining the evaporation-induced precipitation within the regular voids of a colloidal crystal comprising 140 nm sized polystyrene spheres. Post-synthesis removal of the latex and surfactant templates by extraction produced a hierarchically ordered organo-functionalised silica meso–macrophase. FTIR and UV–vis diffuse reflectance spectra indicated the intact and covalent link of chromophore groups into the mesostructured silica network of the hierarchical structure. This method is also extended to many other organosilane moieties tailored to specific applications such as selective chromatographic supports for combinatorial chemistry, ferrocene-based devices in electrochemical sensors, dye-based pH sensors, and rhodium/ruthenium-based organometallic complexes for catalysis.[21] And highly dispersed polyoxometalate clusters could also be incorporated in the hybrid structures of 3D ordered macroporous silicas with mesoporous walls during direct synthesis, and these functionalized materials were demonstrated to exhibit catalytic activity for the epoxidation of cyclooctene with an anhydrous H_2O_2/*t*-BuOH solution at room temperature.[28]

Sen *et al.*[29] synthesized a series of hierarchically ordered porous silica composites with ordering on three different scales of pore size by using latex spheres and triblock copolymers (Pluronic F127 and P123) as templates in the presence of cosurfactants (n-alcohols) in an acidic medium. The silica materials consist of three-dimensional ordered macropores (200–800 nm) with interconnecting, uniform-sized (70–130 nm) windows, and the walls of these macropores consist of mesostructured pores (3–8 nm), as well as a significant microporosity (<2 nm), presenting a macro–meso–microporous structure with a three-dimensional interconnectivity. The formation of windows is due to the close-packed arrangement of polystyrene spheres (touching points). The meso- and microporosity is generated by the micelle formation of the EO–PO–EO block copolymer in the

presence of cosurfactant butanol or pentanol. The surface area and mesopore volume of the materials were low (46 m^2 g^{-1}, 0.053 cm^3 g^{-1}) when the polystyrene latex was removed by direct calcination at 550 °C, while a high total surface area of 531 m^2 g^{-1} was obtained after removal of the latex by toluene extraction followed by calcination at 450 °C.

Ionic liquids, a variety of organic salt having a low melting point and a wide range of liquidus temperatures,[30] have also recently been adopted as templates for the synthesis of mesostructured silicas.[31] In this way, bimodal super-microporous and macroporous silica material was synthesized using PS bead packing and an amphiphilic ionic liquid as dual templates,[32] in which the wall architecture of ordered cubic structure of the macropores is made up of large domains of a practically perfectly ordered supermicroporous (~1.3 nm) lamellar phase surrounding the macropore (~175 nm). Trimodal meso–macroporous silica was prepared using PS beads for macropores, a block copolymer (KLE) for large mesopores, and an ionic liquid (1-hexadecyl-3-methylimidazolium chloride) for small mesopores, respectively (Fig. 3).[33] The macropore size is 360 nm with a wall thickness of 100 nm, and the wall texture of the macroporous silica contains two distinguishable types of pore of different sizes (large spherical mesopores of *ca.* 12 nm and small elongated mesopores of 2–3 nm). No phase separation of block copolymer and ionic liquid was observed, with the small mesopores being located in the walls of the respective larger pores. It is claimed that the synthesis failed with other ionic surfactants such as CTAB. The BET surface area of such trimodal porous silica is 244 m^2 g^{-1}, and the total porosity amounts to *ca.* 0.33 cm^3 g^{-1}.

Further combination of micromolding with PS sphere templating and cooperative assembly of hydrolyzed inorganic species and amphiphilic surfactant/copolymer can lead to the fabrication of hierarchically ordered structures at multiple discrete length scales ranging from ten nanometres to several micrometres.[14] The respective ordered structures can be independently modified by choosing different mold patterns, latex spheres, and block copolymers. The spray-drying techniques,[34] which have been used to process aerosol particles with defined shape and size, can also be used to produce nanocrystalline transition-metal oxide spheres such as TiO_2, ZrO_2, CeO_2 and mixed oxides with controlled multi-scale porosity for many potential applications.[35]

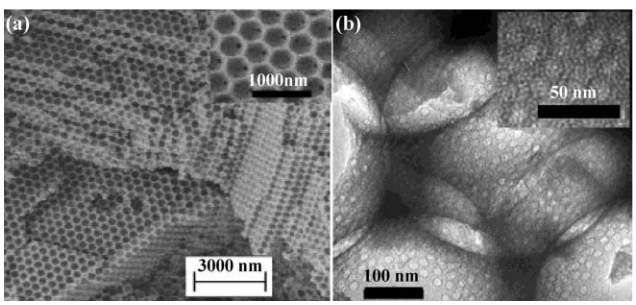

Fig. 3 (a) SEM and (b) TEM images of the trimodal porous silica materials templated by PS spheres, a block copolymer KLE, and an ionic liquid C_{16}mimCl.[33]

2.2 Emulsions, vesicles and bubbles as macrotemplates with combination of supramolecular templating

The method of emulsion templating[36] is perhaps most general and has been used to produce macroporous titania, silica and zirconia with pore sizes from 50 nm to several micrometres, although most of those reported are a disordered macroporous solid without meso- or microporosity. Because the emulsion drops are deformable, macroscopic samples are able to accommodate stresses that arise during gelation and shrinkage. Samples made using rigid spheres, by contrast, tend to break into small pieces that are seldom larger than a few hundred micrometres. In addition, emulsification conditions can be adjusted to produce droplets with different mean sizes which are typically in the micrometre range. Moreover, this can be done to a large extent independently of the self-assembling block copolymer species used to direct the structure of the mesopores. This allows direct and independent control of macro- and mesopore dimensions, so the final pore structures can be tailored to different diffusion and reaction conditions.

Introduction of mesoporosity in a macroporous structure has been reported by a surfactant emulsion-mediated synthesis.[37] The room-temperature synthesis of a macro–mesoporous silica material during the natural creaming process of an oil-in-water emulsion containing surfactant (CTAB) is reported.[37b] The material has three-dimensional interconnected macropores with a strut-like structure similar to meso-cellular silica foams with mesoporous walls of worm-hole structure, *i.e.* macro-cellular foams, which have a high surface area of about 800 m^2 g^{-1} with narrow mesopore size distribution. However, their formation mechanism has not been properly understood. It is also demonstrated that mesoporous silica could be obtained using either a low oil (mesitylene) concentration with slow stirring or synthesis at alkaline pH, while faster stirring at low oil concentration produced meso-cellular silica foam.[37a] Disordered macro–mesoporous silica composites with various wall thickness and interconnectivity were obtained using intermediate to high oil concentration.

Cooper and co-workers reported the synthesis of hierarchically porous emulsion-templated polymer/silica composite beads by sedimentation polymerization of a high internal phase emulsion (HIPE).[38] High surface area silica beads with an average bead diameter of 1.34 mm, high pore volume of 5.68 cm^3 g^{-1} and interconnected macropore structure were obtained by calcinations of the composite structures. Carn *et al.* reported a simple method to prepare porous silica monoliths, hierarchically textured, with organized vermicular-type mesoporosity by the use of a double template, *i.e.* direct emulsion at the macroscale and micellar templates at the mesoscale.[39] The monolithic materials had typical polymerized high internal phase emulsion (poly-HIPE)-type interconnected macroporous textures with polydisperse cell and window sizes within the micrometre range (Fig. 4). Their texture was tuned by varying either the pH of the continuous aqueous phase, the emulsification process or the oil (dodecane) volume fraction. pH conditions have been shown to be an important factor in controlling the final monolith textures, also the oil-water interface seems to promote the inorganic condensation process.

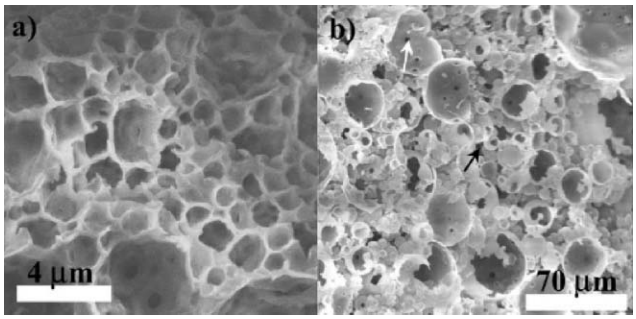

Fig. 4 SEM images of the poly-HIPE-templated macrostructured monolithic silica materials: (a) 1Si-HIPE0.5 and (b) 1Si-HIPE0.035.[39] The black arrow shows an example of the so-called ''external junction'' and the white one shows a typical cell window.

Mesostructured titania having an unusual interior macroporous structure, synthesized in an ethanol solution of surfactant $C_{16}(EO)_{10}$ containing small quantity of preformed water, was spontaneously generated (Fig. 5).[40] The resulting particles have quite a thick shell and a core having a sponge-like macroporous structure with a uniform pore size gradient, such that the macropore sizes increase progressively from the shell layer to the core. Both the shell layers and the macroporous framework of the core have a disordered wormhole-like mesoporous structure of TiO_2 nanoparticle assembly. It is proposed that this hierarchical structure might be formed by combining a reverse micelle (''quasi-reverse-emulsion''[41]) templating pathway with a conventional surfactant templating technique of a hybrid composite mesostructured phase. Moreover, in an aqueous system of amine, by adding an amount of NaCl to a niobium ethoxide/amine, gel vesicle templating of a macro–mesoporous niobium oxide could be achieved (Fig. 6).[42] The salt was emphasized to be necessary for surfactant vesicle formation before the creation of macro–mesoporous niobium oxide with the macropore sizes in the 200–300 nm range, and the process was regarded as a ligand-assisted vesicle templating strategy. The macropore sizes of these niobium oxides were not altered by the preformed vesicles of different sizes, suggesting a

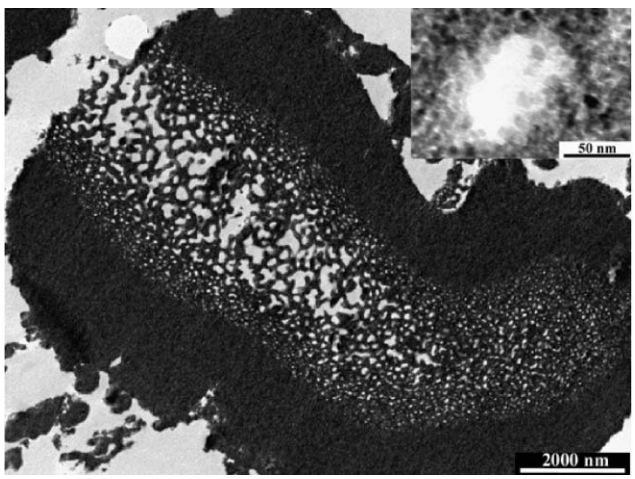

Fig. 5 Cross-section TEM images of hierarchically mesostructured titania with an interior macroporous structure.[40]

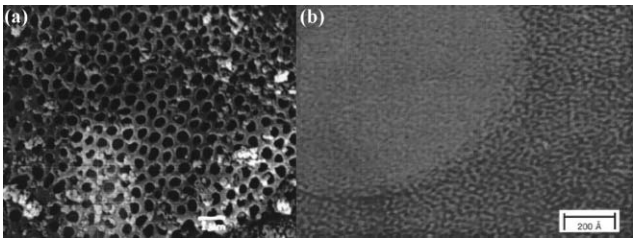

Fig. 6 (a) SEM and (b) TEM images of macroporous Nb-TMS1 synthesized with dodecylamine in an ethanol, salt and water mixture showing uniform macroporosity in the 200–300 nm range and mesoporosity between macropores.[42]

cooperative macropore assembly mechanism rather than one involving performed vesicles.

Macroskeletal mesoporous silicate foams with open-cell random-shaped macrovoids on the (sub)millimetre scale have been prepared from metastable PEO-surfactant air–liquid foams induced by strong stirring under neutral aqueous conditions.[43] It was claimed that the macroscale morphologies were tuned by changing the turbulence of the reaction media, which is certainly a very difficult parameter to control. Since then, a bubbling process has been proposed to produce air–liquid foams,[44,45] which may allow complete control over the cell sizes and shapes of the bubbles and a more easily maintained liquid fraction of the foam. Silica scaffolds with vermicular-type mesoporosity were obtained by this air–liquid foaming sol-gel process where nitrogen was bubbled through a mixture of a surfactant and sol–gel precursor,[44a] while the TiO_2 macrocellular scaffolds obtained had poor mesoporosity arising from the void space induced by the random aggregation of nanoparticles within the foam walls.[44b] Macroscopic cell morphologies were tuned by changing the air/liquid : foam ratios and the size of the nitrogen bubbles, while wall topologies were varied by changing surfactant. Spraying aqueous siliceous solutions containing alkyltrimethylammonium surfactants under high pH conditions resulted in mesoporous silica foams with hierarchical trimodal pore structures (macrovoids and two kinds of mesopores of around 3 and 40 nm).[45] The macrocellular structure was produced with air bubbles, which was stabilized through a rapid condensation reaction during drying. The bimodal mesopore distribution was derived from the surfactant micelles and the interparticle spaces of silica nanoparticles (Fig. 7). This hierarchical architecture of the mesoporous silica foams, having extremely low bulk density (<0.01 g cm^{-3}), high mesopore volume (>2 cm^3 g^{-1}) and specific surface area (>1000 m^2 g^{-1}), is attributable to the self-assembly of air bubbles, surfactant-siliceous complexes and mesostructured silicate particles during the spraying, condensation and drying processes, respectively.

2.3 Polymer membranes and foams as macrotemplates employed with supermolecular porogens

Cellulose acetate and polyamide membranes have been used as templates for the formation of macroporous oxide networks.[46] Infiltration of the silica/amphiphile solution in the porous structure of these membranes and gelation results in a cast of

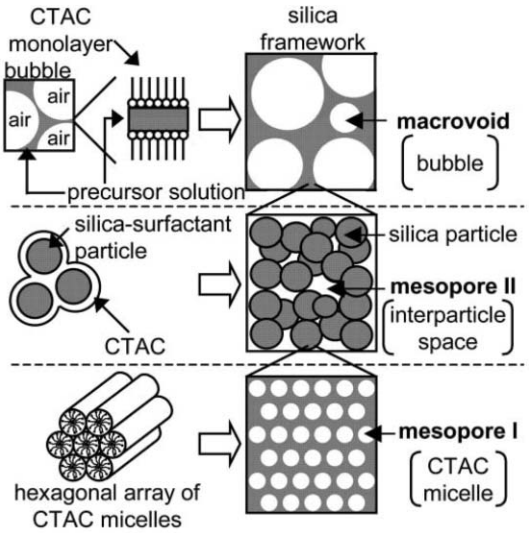

Fig. 7 A schematic model for the hierarchical trimodal pore structure of silica foams by a bubbling process.[45]

the original membrane. Removal of both the membrane template and the porogen of amphiphilic supramolecular aggregates by calcination leaves the amorphous silica film with a bimodal, interconnected meso–macroporous structure (Fig. 8).[47] The surface area and total pore volume of the inorganic films vary from 473 to 856 $m^2\ g^{-1}$, and 0.50 to 0.73 $cm^3\ g^{-1}$, respectively, depending on the choice of template and porogen. The channel-like macropore assembly gives good mass transport and accessibility of the pore systems, whereas the mesopore system provides the large surface area required for catalysis and separation. Other membranes of cellulose derivatives including cellulose nitrate, mixed cellulose esters, and regenerated cellulose can also be applied as templates for the fabrication of bicontinuous macroporous inorganic oxide films with controlled geometry.

Furthermore, applying an external electric field to a polyacrylamide hydrogel could lead to the creation of a template matrix with aligned interstitial voids of approximately 10 μm in diameter. The mesoporous silica monoliths with oriented macroporous channels were then produced by immersion of this electronic-field-oriented hydrogel monolith in neat tetramethylorthosilicate, and subsequent hydrolysis, condensation,

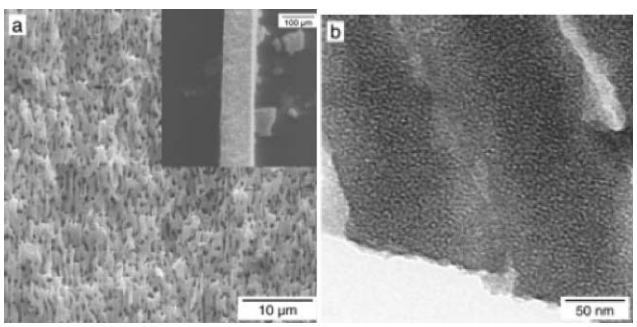

Fig. 8 (a) SEM and (b) TEM images of the meso–macroporous silicas obtained using cellulose acetate membrane and polyoxyethylene (10) lauryl ether ($C_{12}E_{10}$) porogen.[47]

and calcination to remove the organic phase.[48] The mesoporosity was supported by a nitrogen-adsorption isotherm of type IV with a distinct hysteresis loop of type H3, characteristic slit-type pores with average pore diameter 8.6 nm resulted from the aggregation of plate-like particles. The material has a low density of 0.806 g cm^{-1} and a BET surface area of 337 $m^2\ g^{-1}$ with pore volume of 0.73 $cm^3\ g^{-1}$.

Preformed polymer foams are also good candidates for templating macroporous structures. Monolithic polystyrene foams, preformed by polymerization of styrene either in the continuous or the dispersed phase of highly concentrated water/oil emulsions, have been used to synthesize meso/macroporous inorganic oxide monoliths by imbibition of a self-assembling block-copolymer/sol–gel mixture.[49] After calcination to remove the organic components, the resulting meso–macroporous silica, titania, and zirconia materials retained their macroscopic shapes and possessed independently adjustable meso- and macropore structures. The meso–macroporous silica monoliths prepared from the W/O-polystyrene foams and PEO–PPO–PEO triblock copolymer species consisted of cellular macropores 0.3–2 μm in diameter, interconnected by windows approximately 0.2–0.5 μm in diameter with a wall thicknesses of approximately 100 nm, and the highly ordered mesopores of 5.1 nm in size. Alternatively, preformed mesoporous silica nanoparticles were used as building blocks to coat polyurethane foam, leading to mineralization of the foam, and subsequent elimination of the organic foam by calcination resulted in monolithic macrocellular silica foams with a trimodal pore system (small mesopores–large mesopores–macropores).[50] Textural large–mesopores/macropores (in the 20–70 nm range) have their origin in the inter-particle voids, and the small intra-particle mesopore system (2–3 nm in diameter) is due to the supramolecular templating effect of the surfactant.

2.4 Bio-cellulose and starch gel as macrotemplate

For the preparation of porous inorganic materials with hierarchical structures, a rich variety of biological structures with complex morphologies have been used as sophisticated templates. Typical examples of natural biological templates include bacterial threads,[51] echinoid skeletal plates,[52] eggshell membranes,[53] insect wings,[54] pollen grains,[55] plant leaves,[56] and wood celluloses.[57] Since these natural biological templates offer beautiful and abundant hierarchical architectures, and are inexpensive and environmentally benign, they have attracted much interest to construct novel hierarchical inorganic materials.

The bacterial superstructure, consisting of a thread of coaligned multicellular filaments of Bacillus subtilis, was used to extend the length scale of inorganic materials patterning by template-directed mineralization of the interfilament spaces, and ordered macroporous fibres of either amorphous silica or ordered mesoporous silica MCM-41 were produced.[51] The inorganic macrostructures consist of a macroporous framework of 500 nm wide channels with curved walls of either silica or mesoporous silica, 50–200 nm in thickness, showing a structural hierarchy on both the mesoscopic and macroscopic length scales.

Natural wood has highly anisotropic cellular structures, which can be used as a hierarchical template to generate porous ceramics by deposition of a ceramic phase within the wood interstices or infiltration of the ceramic into the unoccupied void space.[57] Mineralization of wood cellular structures using a surfactant-templated sol–gel solution at different pH values allows formation of either positive or negative replicas with hierarchy. At low pH, silicic acid is coated onto the inner surface of the wood cellular structure and it penetrates pores from which degraded lignin and hemicellulose are leached out, to form a positive replica, while at high pH the precipitating silica particles clog the cells and pit structures due to fast condensation, forming a negative replica of wood.[57a] The cell walls consist of surfactant-templated ordered hexagonal mesopores. Moreover, wood was also used as both a carbon precursor and a hierarchical template for silicon carbide synthesis. Mineralized wood with silica in acidic conditions followed by carbothermal reduction in argon resulted in the formation of hierarchical SiC with wood cellular structures.[58] All wood cellular structures were generally maintained and wood cell walls were composed of crystalline SiC nanoparticles (200–700 nm). The specific surface area of the final cellular SiC ceramics was 60–100 m^2 g^{-1}, where the pore sizes were randomly distributed from nanometres to micrometres. Wood cellular structures of SiC materials were stable up to 1400 °C in air.

The cuttlebone is a highly organized internal shell structure constructed from aragonite ($CaCO_3$) in association with a chitin organic matrix. The shell has a chamber-like architecture in the form of mineralized sheets arranged in parallel layers and separated by S-shaped pillars, and has been shown to template ordered chamber-like macroporous chitin–SiO_2 composites.[59] Using chitosan as a template, mesoporous–macroporous siliceous fibrous material could be synthesized *via* hydrothermal hydrolysis of sodium silicate,[60] although the siliceous walls of macropores (570 nm in radius) were micro–mesoporous with a broad and polymodal distribution. This structure may be due to the aggregation of the hydrated chitosan helices in bundles of parallel fibres with different sizes and the gelation of the system.

Starch gel templating was also performed to produce hierarchically spongelike micro–meso–macroporous monoliths of silicalite[61] and meso–macroporous TiO_2,[62] where the macroporosity was generated by self-assembled nanoparticle building blocks. Non-ordered macropores in the size range 0.5–50 μm were achieved by varying the amount of starch and the starch : silicate ratio. Hierarchical macroporous spongelike monoliths and thin films can be obtained with the use of starch gels and sponges.

The use of dextran as a sacrificial template makes it possible to fabricate metallic and metal oxide sponges.[63] By heating pastes of the polysaccharide dextran containing metal salts to temperatures between 500 and 900 °C, self-supporting macroporous frameworks of silver, gold and copper oxide, as well as composites of silver/copper oxide or silver/titania were prepared. Magnetic sponges were similarly prepared by replacing the metal salt precursor with preformed iron oxide (magnetite) nanoparticles.

2.5 Inorganic salt and ice crystals as macrotemplates in combination with supramolecular templating

Spongelike silica membranes with 3D meso–macrostructures have been synthesized by a multiphase process of acid-catalyzed silica sol-gel chemistry in the presence of inorganic salts and self-assembling block copolymers.[64] Inorganic salts play an important role in the formation of the meso–macro silica structures that are grown at the interface of inorganic salt solution droplets. The meso–macrostructured silica network can be varied, depending on the electrolyte strength of the inorganic salts and the amphiphilic block copolymer structure-directing agents. The macropore dimensions are established by the sizes of the salt solution droplets, such as NaCl, LiCl, KCl, NH_4Cl, or $NiSO_4$, which can be adjusted by regulating the evaporation rate of the solvent. At the interstices separating the electrolyte droplets, amphiphilic block copolymer species assemble in the presence of silica to form well-ordered composite mesophases. The morphology of the silica membrane can be modified by changing the concentration of the inorganic salt, although inorganic salt crystals were inevitably co-grown with the silica membrane.

It is very interesting that a method was developed by Nishihara *et al.* to prepare ordered macroporous silica, a silica gel microhoneycomb (SMH), using of micrometre-sized ice crystals as a template.[65] This is based on the phenomenum that when hydrosols, hydrogels, or aqueous slurries of metal oxides or polymer are quickly frozen by immersing them into a cold bath, micrometre-sized ice spheres grow inside their matrices as a result of thermally induced phase separation, and then these ice spheres play the role of a template in the formation of 3D interconnected macroporous metal oxides or polymers. When precursor hydrogels, which are freshly gelled and contain an adequate quantity of solid components, are unidirectionally frozen under a condition where pseudo steady-state growth of ice crystals can continue, an array of polygonal ice rods with fairly uniform diameters grows parallel to the freezing direction. After the removal of the template ice, large monolithic materials with ordered macropores are obtained (Fig. 9). The straight macropores have a polygonal cross section and are parallel to the freezing direction. Besides their ordered macroporosity, micro- and mesopores develop inside the honeycomb walls through the freeze-drying of SMHs soaked in *tert*-butyl alcohol. It was found that the macropore size of the SMHs can be controlled by changing the immersion rate into a cold bath and the freezing temperature, without changing the micro- and mesoporosity of their honeycomb walls. The thickness of the honeycomb walls was

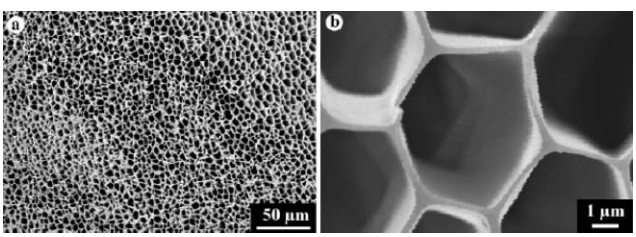

Fig. 9 SEM images of the cross sections of silica gel microhoneycombs prepared by ice-templating.[65]

affected by the SiO_2 concentration and the macropore size. The porosity of the honeycomb walls could be controlled to be microporous as well as mesoporous by hydrothermal treatment of as-prepared SMHs in basic aqueous solutions. Moreover, SMHs with developed mesopores showed a higher stability against heat treatment.

2.6 Polymerization induced phase separation in the presence of polymers

Chemically induced liquid–liquid phase separation has been applied in the synthesis of siliceous mesoporous materials with co-continuous macropores.[66] This technique is based on the hydrolysis and condensation of inorganic precursors in the aqueous domain of a microphase-separated medium, derived from the self-assembly phase of the template used. A wide variety of water-soluble polymers, such as poly(ethylene oxide), has been used to control the phase separation/gelation kinetics in the preparation of monolithic silica of virtually any shape exhibiting both interconnected macropores and textual mesoporosity. With use of various Si precursors such as tetramethoxysilane, tetraethoxysilane, and bis(trimethoxysilyl)-ethane, amorphous or disordered mesopores can be embedded in gel networks which constitute a co-continuous macroporous structure.[67] The phase separation is driven by the repulsive interaction between the hydrophobic PEO–oligomer complex and the hydrophilic solvent. The macroporous morphology is the result of phase separation that took place earlier than the sol–gel transition. The walls in this macroporous structure consist of aggregates of silica nanoparticles giving rise to textural mesoporosity in the walls with pore sizes in the 10–20 nm range and a high surface area. Poly(ethylene glycol) used together with alkylammonium surfactant was found to better control the particle aggregation and internal structure of silica monoliths with hierarchical meso–macroporosity,[68] although the ordered mesopores were still difficult to obtain and detect by XRD diffraction. Alkoxide-derived alumina–silica[69] and silica–zirconia[70] a having meso–macroporous structure can also be synthesized by this technique in the presence of polyethylene oxide, however, the formation of a 3D interconnected macroporous structure was seldom achieved in transition-metal alkoxide-derived sol–gel systems.[71] This is because the transition-metal alkoxides are very reactive toward hydrolysis, and it is generally difficult to control the structural development until gelation. The maximum quantity of Al^{3+} required is only 10 mol% to obtain macroporous alumina–silica gels.[69]

Monolithic macro–mesoporous ethanesilica[72] and pure silica[73] gels have also been synthesized *via* polymerization-induced phase separation in the presence of the block copolymer P123 and a micelle-swelling agent 1,3,5-trimethylbenzene. The addition of a micelle-swelling agent was found to induce the mesostructural transformation from 2D-hexagonal order to mesostructured cellular foam, accompanied by minor modification or even without disturbing the macroporous framework structure. The orderliness of the mesostructures was confirmed by FE-SEM and XRD. Whereas, Shi *et al.*[74] synthesized the silica monolith with textural pores and ordered mesopores, similar to the ethanesilica based monolith reported by Nakanishi *et al.*,[72,73] by a sol-gel process using the triblock polymer F127 as a pore directing reagent, where F127 demonstrated its dual functions of phase separation and meso-templating, and found that the ordered hexagonal mesopores in the silica skeletons, observed in TEM images but not supported by XRD patterns, was not connected.

Considering that short-chain alcohols generated by the hydrolysis reaction of metal alkoxides generally disturb the self-organization of structure-directing agents, leading to the disordering of the mesostructures of the product, several efforts have been devoted to organize a highly ordered mesoporous gel network into macroporous assemblies. The undesired co-presence of short-chain alcohol in the meso-structure-forming stage could be avoided by the modification of the starting alkoxide, and hierarchical porous silica network built up from periodic interconnected mesoporous silica strands was synthesized (Fig. 10).[75] Using the ethylene glycol- and propane-1,2-diol-modified silanes as inorganic precursors and an amphiphilic triblock copolymer as structure-directing agent,[76] silica monoliths exhibiting a unique hierarchical network structure with a bimodal pore size distribution in the macro- and mesopore size regime and high surface areas were prepared by phase separation on different levels. In addition to an extraordinary cellular network structure with interconnected macropores of several hundreds of nanometres in diameter, the material exhibits a well-ordered mesostructure with periodically arranged mesopores of about 6–10 nm in diameter. However the application of glycerol-modified silanes resulted in the formation of a disordered silica mesostructure. The modified silane offers two major advantages compared to the conventionally used TEOS and tetramethoxysilanes: the precursor is water-soluble and thus allows a direct mixing with

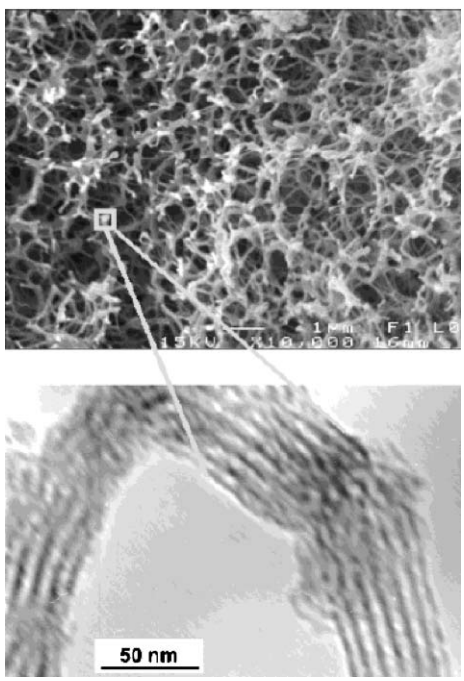

Fig. 10 SEM (top) and TEM (bottom) of a macro–mesoporous silica monolith synthesized with ethylene glycol-modified silane as an inorganic precursor and the triblock copolymer P123 as a meso-template.[75a]

the lyotropic liquid crystal like phase of the block copolymer in water; second, it does not require a catalyst to start the hydrolysis and condensation reactions.[75a] The ethylene glycol, released during the hydrolysis and condensation reactions, is not detrimental to most of the liquid crystal surfactant mesophases.

2.7 Self-assembly in the presence/absence of surfactant

It has been found that hierarchical meso–macroporous metal oxides can be synthesized even without the need for any macrotemplates such as latex spheres, emulsions, foams, or polymer-induced phase separations.[77–83] The initial work was done on the zirconia,[78,79] alumina,[80,81] titania and binary mixed oxides[82,83] *via* the hydrolysis from the corresponding metal alkoxides in the presence of a single surfactant (either cationic or non-ionic surfactant), and the synthesized materials exhibit a parallel-arrayed channel-like macroporous structure, generally having a dense layer on the face of the monolithic particles under the end of macrochannels (Fig. 11). The macroporous framework is composed of accessible mesopores with a wormhole-like array. The framework walls of aluminium oxides can even be crystalline with boehmite and γ-alumina phases, and their mesostructures were formed through the scaffold-like aggregation and intergrowth of the boehmite and γ-alumina nanofibers, respectively.[81] Such a macromorphology is distinct from the materials obtained by the use of macrotemplate (latex spheres, emulsions, foams or bio-celluloses) or polymer-induced phase separation. The preliminary studies suggested that the single surfactant would direct the formation of inorganic phases with multidimensional pore systems by the formation of vesicle-type supermicelles resulted from the aggregation of unreacted excess surfactants.[78] However, the application of this method to silica was not successful,[80] which may be the effect of the fast hydrolysis rate of the metal alkoxides. This phenomenon contrasts with the case of polymer-induced phase separation.

The recent reports have also revealed that the similar macroporous structure could be spontaneously formed even in the absence of a surfactant,[84–88] although the formation of the macropores required the presence of an alkoxide droplet within the synthesis mixture. The surfactant played no role other than to influence the hydrodynamic conditions during synthesis,[86] which could influence the texture of the final materials. Since the macropore-free layer was observed on one side of the particle coupled with the curvature of the particle, Mann and coworkers[84] proposed a formation mechanism involving the initial formation of a semipermeable membrane on the outside of the alkoxide droplet, which restricted the hydrolysis/condensation domain such that the reaction subsequently moved inward. The formation of the macropore channels was attributed to microphase-separated regions of metal oxide and solvent established by the flow of the solvent across the membrane to the alkoxide interface. Once the macropore channels were formed, they would preferentially propagate toward the alkoxide since it would provide the least resistant path for the water to react at the solution/alkoxide interface. Although this proposed formation mechanism could explain many of the observations, it still appears to leave several outstanding questions.[86] For example, the mean macropore size distribution increased with the solvent Reynolds number,[86] and tubular macrochannels with open tips were often seen in the similar particle synthesis (Fig. 12).[82,85–89]

Porous aluminosilicate materials have been widely used as acid catalysts and supports.[90] The introduction of a hierarchical architecture will enhance their performance further. By using alkoixdes of silicon and aluminum in a controlled aqueous solution, either with or without surfactant, a spontaneous formation of aluminosilicate macrochannels with tunable mesoporous walls occurred. A study on the role of the surfactant molecules revealed that they facilitated the incorporation of aluminum atoms into the silicate framework.[82,85]

The hydrolysis/polycondensation of aluminum sec-butoxide in a mixed solution of H_3PO_4 and Na_2HPO_4 led to the formation of hierarchically phosphated meso–macroporous nanocrystalline aluminum (oxyhydr)oxides, incorporating phosphorus into the framework by the surface Al–O–P

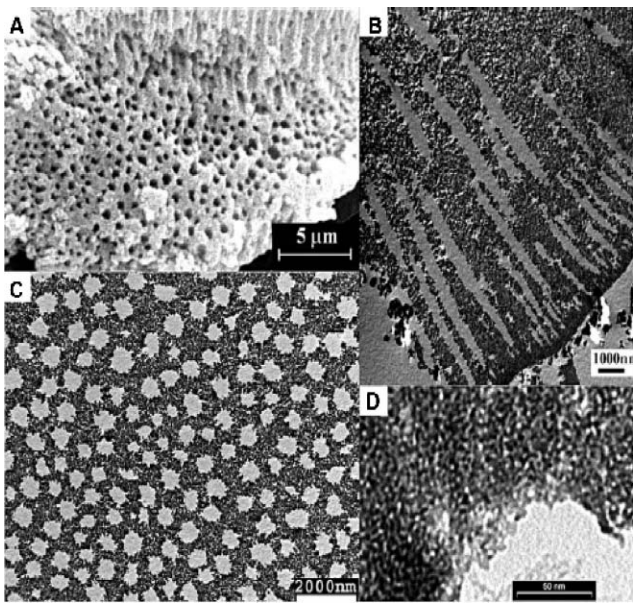

Fig. 11 (A) SEM and (B–D) cross-sectional TEM images of the meso–macroporous zirconia synthesized with one single surfactant, viewing from different directions and with different magnifications.[77]

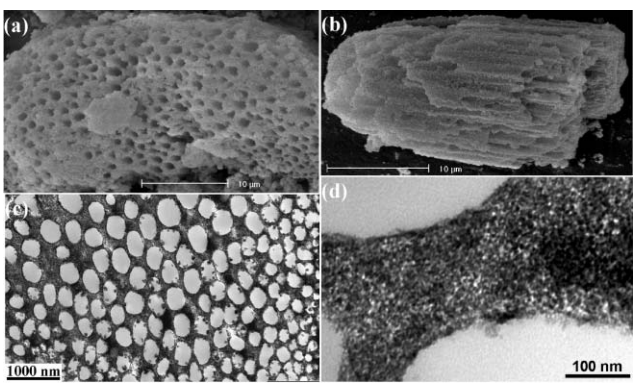

Fig. 12 (a, b) SEM images and (c, d) cross-sectional TEM images of hierarchically macroporous zirconium phosphate with supermicroporous walls spontaneously formed in the absence of surfactant.[87]

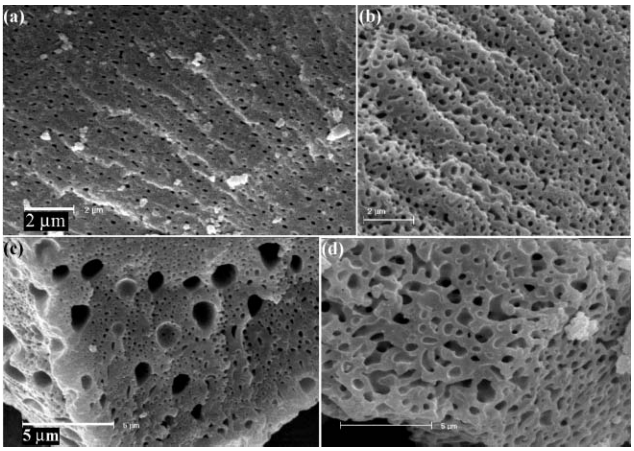

Fig. 13 SEM images of the meso–macroporous titanium phosphates synthesized (a) in the absence of surfactant, and in the presence of (b) 5%, (c) 10%, and (d) 15% surfactant Brij 56.

bonding.[88] Surfactant Brij 56 was found to take no direct role in the formation of either mesoporous or macroporous structures, but to significantly influence the textural properties and porosities of the resultant phosphated aluminum (oxy-hydr)oxides which possessed high thermal stability, high surface areas and large acidity.

Hierarchically meso–macroporous titanium phosphate, obtained by direct hydrolysis of titanium tetrapropoxide in orthophosphoric acid aqueous solution, demonstrated a macroporous structure of 50–160 nm in size with mesoporous walls (Fig. 13a).[91] Addition of a small quantity of nonionic poly(ethylene oxide) surfactant (*e.g.* 5%) led to an improvement in the macroporosity with a slight enlargement of macropore sizes to 80–250 nm (Fig. 13b). A secondary large macropore system with parallel channels of 500–1000 nm in size was obtained when the synthesis was performed with a 10% surfactant content, leading to the bimodal macroporous structure with mesoporous walls (Fig. 13c). Further increase of surfactant quantity resulted in the presence of a uniform three-dimensional co-continuous macroporous structure with accessible wormhole-like mesoporous walls (Fig. 13d). This new series of experiments again highlight the hot discussion on the role of the surfactant molecules during the formation of hierarchical porosity. The precise mechanism underlying these hierarchical materials remains elusive. It is interesting to note that the macrochannel shapes (funnel-like or straight tubular) could be tunable, depending on the synthesis conditions and inorganic source used.[78,79,82,83,87–89]

Chen *et al.*[92] synthesized thermally stable meso–macroporous zirconia with a nanocrystallized framework by using composite surfactants of the amphiphilic block copolymer P123 and poly(ethylene oxide) surfactant Brij56 at a hydrothermal treatment temperature of 130 °C which is considerably higher than the generally reported 60–80 °C.[78–83] The big hydrophobic cores of P123 can adsorb a great number of small-sized hydrophobic groups of Brij56 surfactant molecules. The surplus composite surfactant micelles can aggregate by self-assembly to form "supermicelles" and adsorb onto the hydrophilic solid surfaces, directing the formation of macroporous structures of mesostructured zirconia. Since higher temperatures do not favour the formation of surfactant supermicelles, little macroporous structures were obtained when one single surfactant was used at this elevated temperature. The use of the amphiphilic block copolymer (P123) was believed to be responsible for the improved ordering of the pore structures and the crystallization of the framework without pore structure collapse *via* certain cooperative effects with the small-sized Brij56 surfactant molecules. This result does support the initially proposed formation mechanism.[78,79] Thus, further work is really necessary to reveal the true mechanism of this spontaneous formation process of meso–macroporous materials.

3 Synthesis of meso–macroporous carbons

Porous carbon materials can be easily made by the nanocasting strategy,[93] that is to say, using a replica of porous structured silica materials, where porous silica is impregnated with a carbon precursor, followed by carbonization under non-oxidizing conditions. This is a difficult but efficient templating strategy. The replication of meso–macroporous silica enables the preparation of hierarchical bimodal porous carbon with various shapes, where the macroscopic shape can be controlled through the shape of the silica monolith used as the template structure, and the macropore diameter can be varied between 0.5–30 μm in a controlled manner.[94–96] The carbon monolith is a positive replica of the silica monolith on the micrometre scale, but a negative replica on the nanometre scale. Lindén and co-workers[94,95] reported the hierarchical carbon replica of their meso–macroporous silica,[68] and the meso–macroporous carbon had a BET surface area of over 1000 $m^2\ g^{-1}$ and a specific pore volume of 1.2 $cm^3\ g^{-1}$. A significant microporosity can be obtained in these carbon replicas, leading to the tri-modal porous carbons.[95,96]

Ordered macroporous carbon with mesoporous walls has also been produced by template replication of aggregates of small silica particles, which were themselves templated by a self-assembled lattice of larger monodisperse polystyrene spheres.[97] Fig. 14a shows the SEM images of the silica template composed of silica nanoparticles of about 12 nm in size forming the wall of macropores of about 330 nm in diameter. The voids between the packed silica nanoparticles provide fully interconnected mesopores, which can be impregnated with the carbon precursor divinylbenzene. The carbonization of the carbon precursor and subsequent dissolution of the silica particle framework resulted in bimodal porous carbon replica composed of macropores of about 317 nm in diameter connected to small mesopores of about 10 nm in size (Fig. 14b). Three round holes in the wall appear as black dots with diameters of about 110 nm, through which a macropore is connected to the three neighboring macropores below the macropore in the image. The size of the large macropores can be manipulated by controlling the diameter of the polystyrene spheres, while the size of the small mesopores and the overall specific surface area are determined by the silica nanoparticles. However, this interconnected, ordered, uniform pore structure of carbon material has a relatively low BET surface area of 465 $m^2\ g^{-1}$ with total pore volume of 1.32 $cm^3\ g^{-1}$, which is in comparison to the silica template (106 $m^2\ g^{-1}$, 0.29 $cm^3\ g^{-1}$).

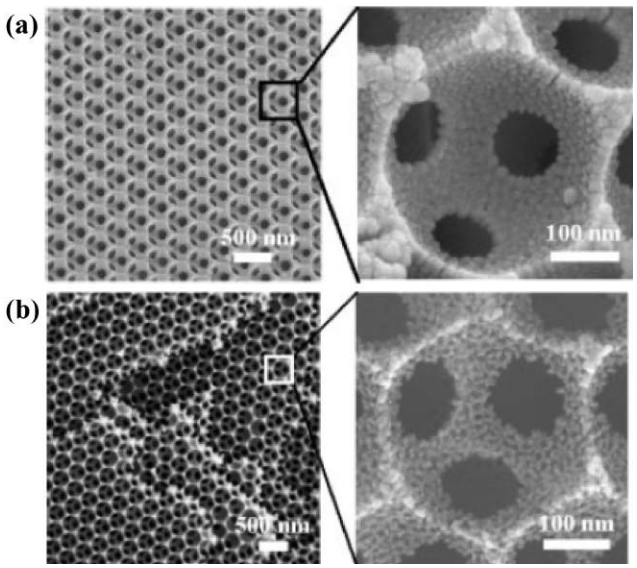

Fig. 14 SEM images at different magnifications of a silica template composed of (a) silica nanoparticles of about 12 nm in size forming the wall of macropores of about 330 nm in diameter, and (b) the resulting bimodal porous carbon replica composed of macropores of about 317 nm in diameter connected to small mesopores of about 10 nm in size. This periodically ordered, bimodal porous carbon is termed POBPC(317-10).[97]

4 Applications for hierarchical materials

Applications for hierarchical meso–macroporous materials are emerging. Many possible applications of multiscale porous materials, combining high diffusion with high surface area and high pore volume ratio, are related to their high accessibility and high storage capacity. In this section, selected applications of meso–macroporous materials are highlighted.

4.1 HPLC Separation

Silica gel particles are extensively used as a packing material of columns for high-performance liquid chromatography, HPLC. Silica monoliths with continuous macropores synthesized *via* the phase-separation route have been used as the stationary phase in HPLC separation and showed much higher performances than conventional columns packed with particles.[98,99] The high column efficiency and low pressure drop in the monolithic columns of bimodal meso–macroporous silica correspond to the features of hierarchical porous silicas, *i.e.* small-sized skeletons with appropriate mesopores and relatively large through-pores (macropore),[99] and these are advantages for high-speed separations. Increased (through-pore size) : (skeleton-size) ratios can result in higher permeability and shorter diffusion path lengths, providing higher efficiency. Both a thinner gel skeleton and higher through-pore volume in the well-defined structure contribute to enhancement of the analytical performance of the monolithic columns under a higher mobile phase velocity. The mesopore sizes could be tailored through post-treatment in ammonia solution in order to access the chromatographically important mesopore-size range of 5–25 nm,[99] and it is found that the larger mesopores of the monolithic silica column showed higher separation efficiency than smaller mesopores.[100] Such a highly permeable and hierarchically porous structure will provide higher column efficiencies for high-molecular-mass solutes with a low diffusion coefficient.

Hierarchical hexagonal mesoporous MSU-type silica prepared with Pluronic P123 copolymer in mild acidity by a two-step process, composed of nanoparticles (200 nm in size) that entrapped microvoids inside the particles, was also tested for HPLC.[101] Although the powder was not optimized for this application, the first results on ungrafted silica appear equivalent to those obtained with a commercial HPLC silica powder. It is expected that by embedding highly ordered mesopores in the gel skeletons constituting the well-defined macroporous framework, a highly efficient liquid-phase contact device suitable for separation, reaction, and sensing purposes, can be prepared.

4.2 Catalysis

The structural features of these meso–macroporous materials promise uses as potential supports and catalysts in heterogeneous catalysis for bulkier molecules where diffusion of reactant molecules could be facilitated. A controlled multiporosity network with a high surface area, the wide variety of oxide compositions, and the ability for homogeneous or selective doping of active sites, are in high demand for improved catalytic activity. Currently the applications in reaction processes are emerging.

Hierarchical porous alumina-silica prepared by polymer-induced phase separation was found to have a large number of Brønsted acid sites effective for the cracking of cumene.[102] The PEO surfactant was believed to increase the uniformity of Al in the silica network and this would cause the formation of Brønsted acid sites, although the effectiveness of the presence of the macropores in the laboratory-scale reactor has not been established yet. The addition of nickel into a phase-separation silica-PEO system allowed the formation of a nickel catalysts dispersed in the mesopores of silica gel skeleton rather than aggregated in macropores.[103]

Heterogeneous acid catalysis may benefit from monolithic meso/macroporous catalysts with independently adjustable mesopore and macropore dimensions and macroscopic morphologies, due to the sensitivity of catalytic reaction rates and selectivities to diffusive resistances to mass transfer. Such considerations have been shown to be important for the low-molecular-weight reactants and products and will play an even greater role for large macro- and biomolecular species. Meso/macroporous solids present opportunities for the hierarchical design and engineering of heterogeneous catalysts with improved control and integration of materials composition, structure, and performance.

Chmelka and co-workers prepared meso–macroporous aluminosilicas (Si/Al = 72) of centimetre sized, mechanically stable monoliths with interconnected macropores whose walls are comprised of ordered mesopores by combining oil-in-water (O/W) emulsion and block-copolymer templating,[104] and investigated their Friedel–Crafts alkylation properties of single-ring aromatic compounds, including toluene, ethylbenzene, cumene, and styrene, with benzyl alcohol. The

toluene alkylation activities of the meso-macroporous monolith catalysts were compared with nanoporous zeolite Beta (Si/Al = 75,) and mesoporous SBA-15 aluminosilica (Si/Al = 70), as powders and pellets. Moderate toluene alkylation rates ($\sim 10^{-4}$ s^{-1}) and in high selectivities (>90%) for benzyl toluene were observed for meso–macroporous aluminosilica SBA-15 monoliths, compared to the mesoporous SBA-15 and zeolite beta powders, which displayed faster alkylation rates ($\sim 10^{-3}$ s^{-1}), though were less selective (79 and 59%, respectively). In pellet form, both the mesoporous SBA-15 and the zeolite beta materials yielded lower rates of alkylation ($\sim 10^{-4}$ s^{-1}), due to slower internal diffusion of reactants and products within the smaller pellet macropores, compared to the meso–macroporous monoliths. The aluminosilica meso–macroporous SBA-15 monoliths deactivated more slowly, retaining 92% of their original activities after one use, compared to 75, 76, and 0.6% for SBA-15 powder, SBA-15 pellet, and zeolite beta powder catalysts, respectively.

Meso–macroporous metal oxides prepared by surfactant-assisted spontaneous assembly[78–81] have also found potential applications in catalysis. The introduction of light-harvesting macroporous channels into mesoporous TiO_2 framework can increase its photocatalytic activity,[105] due to the minimization of intradiffusion resistance and the enhancement of photoabsorption efficiency. The activity of meso–macroporous titania in ethylene photodegradation is much better than that of the Degussa P25 titania. The 350 °C calcined catalyst showed photocatalytic reactivity about 60% higher than that of P25. The synthesized meso–macroporous titanium and zirconium phosphates[87,91,106] have been found to possess a large quantity of acid sites, which should be interesting for catalysis applications. The synthesized meso–macroporous ZrO_2, TiO_2 and ZrO_2–TiO_2 were used as supports for Pd catalysts, and tested for total oxidation of volatile organic compounds (VOCs).[107] These supported Pd catalysts were found to be powerful catalysts for total oxidation of toluene and chlorobenzene, in which Pd/TiO_2 presented the highest catalytic potential.

The $Ce_xZr_{1-x}O_2$ materials with different cerium contents, prepared by the hydrolysis of the mixture of zirconium n-propoxide and ammonium cerium(IV) nitrate in a surfactant solution, have a meso–macroporous structure that could be preserved even at a high cerium content of 60% and after calcination at 800 °C, which was used as a catalyst support of high-efficiency oxidation catalyst Pd/$Ce_xZr_{1-x}O_2$.[108] With increasing calcination temperature, better crystallization of the cubic phase and incorporation of more zirconium into the ceria lattice were observed. The catalytic activity for CO oxidation was better than that obtained from catalysts without macrochannel structures and the one prepared by the co-precipitation method. Such high catalytic efficiency can be explained by the high crystal phase homogeneity, availability of more oxygen vacancies and an enlarged surface area.

4.3 Electrode materials for fuel cell application

The conventional electrode materials of solid oxide fuel cells (SOFCs) such as nickel/yttrium oxide-stabilized–zirconium oxide cermet (ceramic/metal) and perovskite or platinum/yttrium oxide-stabilized–zirconium oxide are usually fairly dense crystalline structures with small porosity and low surface area. Large porosity with high surface area is quite important for these electrode materials in reducing the operating temperature of SOFCs by allowing easy diffusion of gaseous reactants and reducing the barrier for chemisorption by the electrode. Ozin's group have investigated the electroactivity of binary and ternary mesoporous yttria–stabilized-zirconia and metal (Pt, Ni)–yttria–zirconia solid solutions,[109] and interesting oxygen ion and electron charge-transport properties were observed.

By the procedure of spontaneous assembly, mesoporous binary yttria–zirconia materials with an ordered channel-like macroporous structure have been synthesized in our group.[110] This thermally stable hierarchical structure provides large accessibility for gaseous reactants within the pores, enhancing the exchange rates of gaseous reactants by influencing adsorption equilibria and promoting overall charge-transfer reactions at the triple phase boundary that controls the efficiency of the SOFCs, which is thus applicable as a new solid fuel-cell electrode materials.

Ordered and uniform macroporous carbons with mesoporous walls,[97] templated by aggregates of polystyrene spheres and silica particles, have been used as catalyst supports in direct methanol fuel cells (DMFCs). The synthesized periodically ordered, bimodal porous carbon (POBPC), denoted as POBPC(317-10) with a macropore diameter of about 317 nm and mesopore size of about 10 nm, was used as a support material for electrode catalyst Pt–Ru alloys in fuel cells. In comparison with the commercially available E-TEK and Vulcan XC-72 carbon (VC) Pt–Ru catalysts, a significantly improved activity for methanol oxidation was obtained on the POBPC(317-10) Pt–Ru catalyst as an anode in a DMFC unit cell (Fig. 15). As shown in Fig. 15, whatever polarization curves of the DMFC were determined at 30 °C or 70 °C, the POBPC catalyst shows higher current density and maximum power density than those of the E-TEK catalyst. Such a large improvement may be related to the unique structural properties of the POBPC, which are considered to be due to the combination of high surface area and facile fuel and product diffusion. This uniform bimodal meso–macroporous carbon also shows better catalytic activity than the macroporous carbon with an identical ordered-lattice structure but with no designed mesopores in the walls,[111] demonstrating the importance of the small mesopores in the walls, which may add another dimension to high degree of catalyst dispersion.

4.4 Biomaterials engineering and controlled drug delivery devices

Inorganic porous materials are emerging as a new category of host/guest systems of drug delivery.[112] Due to the non-toxicity, chemical inertness and mechanical properties of multi-scale porous materials of silica, alumina and titania, besides their high surface area and high pore volume, these hierarchical porous materials, especially aerosol,[35] are expected to be good carriers for controlled drug loading and release. It has been revealed that the release process is mainly diffusion controlled, depending on the pore connectivity and pore geometry of the materials,[113] and a one-dimensional pore structure with cage

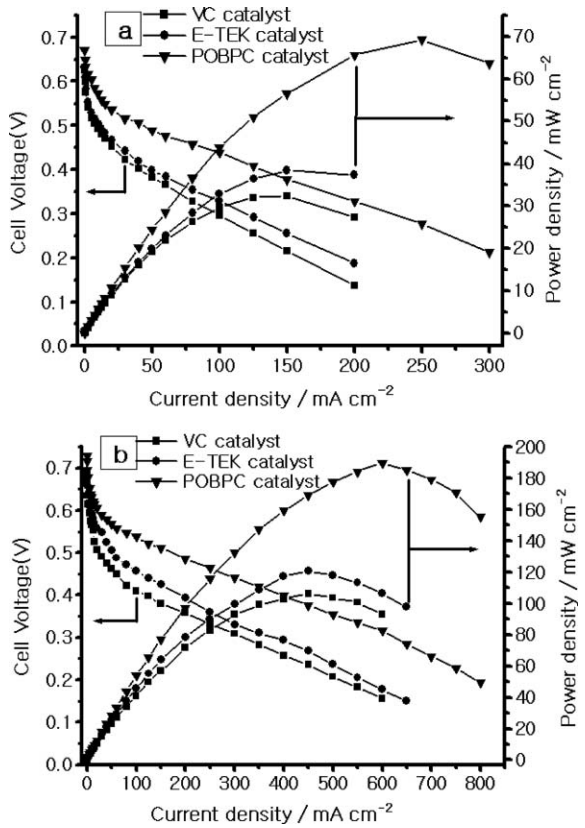

Fig. 15 The polarization curves for a direct methanol fuel cell using a VC Pt_{50}–Ru_{50} catalyst (■), a commercial E-TEK Pt_{50}–Ru_{50} catalyst (●), and a POBPC(317-10) Pt_{50}–Ru_{50} catalyst (▼) determined at (a) 30 °C, and (b) 70 °C.[97]

like pores was found to be the most promising pore geometry for providing a slow release of drugs from mesoporous hosts. Furthermore, the hierarchically ordered meso–macroporous silica materials can also be used as a host for loading biomolecules such as enzymes.[114] The immobilized enzyme reactors developed are expected to be suitable for various enzyme applications such as bioremediation, biosensors, and bioconversion. It has been found, by the study of the lysozyme immobilization on several silica supports (bimodal porous silica UVM-7 and conventional silica xerogels), that the loading amounts can be correlated to the open nature and accessibility of the internal surface area.[115] Bimodal UVM-7 silicas have a very quick adsorption rate and high enzyme loading.

Hierarchical meso–macroporous materials are also interesting for tissue engineering. An α-tricalcium phosphate porous body of bioabsorbable ceramic with a continuous macroporous (10–50 μm) structure,[116] synthesized by a conventional sintering procedure using a slurry composed of β-tricalcium phosphate and potato starch, is attractive for bone fillers in medical applications because the porous structure of macropores allows cell invasion. An increased surface area of the porous body is also required to increase the volume of drugs or osteoinductive factors that are incorporated into the porous body, which can be achieved by the formation of addition small pores (mesopores). Chemical treatment of the α-tricalcium phosphate macroporous ceramic scaffold with a buffered solution at pH = 4 resulted in the formation of mesopores with a remarkable increase in surface area of the scaffold, and the precipitation of octacalcium phosphate. Such bimodal meso–macroporous distribution brought about higher adsorption of bovine serum albumin, acidic protein, than with a monomodal pore size distribution of mesopores,[117] giving high ability drug carriers.

4.5 Membrane reactors

Thin films and membranes of hierarchically meso–macroporous silica have been synthesized by using appropriate macrotemplates such as polymer membranes,[47] colloidal crystals, and inorganic salts[64] and amphiphilic supermolecule mesotemplates. They may find applications in areas of large molecule (biomolecule) separation and catalysis.[118] Enhanced gas and liquid flow rates through such membranes, due to the presence of the larger pores, also make them attractive as supports for other catalytic materials. The recently reported hierarchical meso–macroporous metal oxides synthesized with one single surfactant have a aligned funnel-like macroporous structure perpendicular to one dense layer face,[78] which can be applicable as semipermeable membranes for process filtration, cell culture, or laboratory filtration, as well as one-pot reactors.

5 Conclusions and outlook

It has been demonstrated that hierarchical meso–macroporous materials with various porous structures and pore scales can be prepared by several methods involving the use of supermolecular assembly of amphiphilic polymers and surfactants employed with the macrotemplates such as colloidal crystals, polymer foams, bio-celluloses, emulsions, inorganic salt and ice crystals, by macroscopic phase separations or by innovative self-generation processes. In the most synthesis methods, both the macroporosity and mesoporosity can be easily and independently adjusted. The internal mesostructures are generally decided by the co-operative self-assembly of amphiphile supermolecules and inorganic precursors, while the macroporous structures are controlled by the nature of the selected macrotemplates. Furthermore, the macroscopic morphology can also be designed to be of monoliths, thin films, membranes or spheres, depending on the the demands of various practical applications. The hierarchical materials synthesized with interconnected bimodal meso–macroporous structures and defined morphologies can be expected to combine reduced resistance to diffusion and high surface areas for adsorption and reaction, particularly for large molecular guest species (*e.g.* bio-molecules).

However, the design of such multi-scaled porous materials with controllable ordered pore structures and crystalline framework still remains a challenge. The structural stability and framework crystallinity may also be important issues for these hierarchical materials, regarding their practical applications. The formation mechanism of spontaneous assembly of the hierarchical meso–macroporous metal oxides is still not totally clear to date. The development of new and versatile synthesis methods is still interesting and necessary. Moreover, utilizing these meso–macroporous oxide materials as templates to make replicas of hierarchical carbon or other composites is

attracting much attention and would be a new and interesting research direction.

Nature is a unlimited specimen with numerous examples of exceptionally strong building materials. Despite their diversity, one nearly constant feature is that almost all biomineralized structures are enormously hierarchical. These materials often show complex hierarchical organization from the nanometre to macroscopic scale, teaching us how structural materials can assemble themselves. Nature, supplying multiple lessons of self-formation of hierarchy, is therefore the source of inspiration for new strategies.[119,120]

The combination of multi-scaled porosity integrated into one moldable body has promise for yielding improved overall reaction, adsorption/separation, and/or structural properties. Some practical applications of these attractive meso–macroporous materials have been emerging, including HPLC separation, catalysis, fuel cell electrode materials, biomaterials engineering, controlled drug delivery devices, and membrane reactors. The enhanced performances in catalysis, adsorption and separation have been achieved in these hierarchical porous materials, and can be attributed to the minimization of intradiffusion resistance and the high surface area for activate site dispersion. Moreover, their intriguing properties can grant the extension of applications to gas sensing,[121] since the multiscale porous architecture promotes gas diffusion and increases the active surface area.[122] It is reasonable to expect that further modification of the individual porosities and intricate morphologies, as well as surface functionalization, of the meso–macroporous materials may open new perspectives for application when considering combined properties.

Acknowledgements

This work was supported by the European Program of InterReg III (Programme France-Wallonie-Flandre, FW-2.1.5) and realized in the framework of the Belgian Federal Government PAI-IUAP 01/5 project.

References

1 (*a*) A. Stein, *Adv. Mater.*, 2003, **15**, 763; (*b*) M. E. Davis, *Nature*, 2002, **417**, 813.
2 G. J. A. A. Soler-Illia, C. Sanchez, B. Lebeau and J. Patarin, *Chem. Rev.*, 2002, **102**, 4093.
3 (*a*) C. T. Kresge, M. E. Leonowicz, W. J. Roth, J. C. Vartuli and J. S. Beck, *Nature*, 1992, **359**, 710; (*b*) J. S. Beck, J. C. Vartuli, W. J. Roth, M. E. Leonowicz, C. T. Kresge, K. D. Schmitt, C. T.-W. Chu, D. H. Olsen, E. W. Sheppard, S. B. McCullen, J. B. Higgins and J. L. Schlenker, *J. Am. Chem. Soc.*, 1992, **114**, 10834.
4 (*a*) D. Zhao, J. Feng, Q. Huo, N. Melosh, G. H. Fredrickson, B. F. Chmelka and G. D. Stucky, *Science*, 1998, **279**, 548; (*b*) D. Zhao, Q. Huo, J. Feng, B. F. Chmelka and G. D. Stucky, *J. Am. Chem. Soc.*, 1998, **120**, 6024.
5 (*a*) B. T. Holland, C. F. Blanford and A. Stein, *Science*, 1998, **281**, 538; (*b*) C. F. Blanford, H. Yan, R. C. Schroden, M. Al-Daous and A. Stein, *Adv. Mater.*, 2001, **13**, 401; (*c*) H. W. Yan, C. F. Blanford, B. T. Holland, W. H. Smyrl and A. Stein, *Chem. Mater.*, 2000, **12**, 1134.
6 J. Fan, C. Yu, J. Lei, Q. Zhang, T. Li, B. Tu, W. Zhou and D. Zhao, *J. Am. Chem. Soc.*, 2005, **127**, 10794.
7 (*a*) J. Yu, J. C. Yu, M. K.-P. Leung, W. Ho, B. Cheng, X. Zhao and J. Zhao, *J. Catal.*, 2003, **217**, 69; (*b*) N. Tsubaki, Y. Zhang, S. Sun, H. Mori, Y. Yoneyama, X. Li and K. Fujimoto, *Catal. Commun.*, 2001, **2**, 311.
8 Z. Y. Yuan, J. L. Blin and B. L. Su, *Chem. Commun.*, 2002, 504.
9 S. A. Bagshaw, *Chem. Commun.*, 1999, 1785.
10 X. Wang, T. Dou and Y. Xiao, *Chem. Commun.*, 1998, 1035.
11 J. Sun, Z. Shan, T. Maschmeyer, J. A. Moulijn and M.-O. Coppens, *Chem. Commun.*, 2001, 2670.
12 J. E. Haskouri, D. O. de Zarate, C. Guillem, J. Latorre, M. Caldés, A. Beltran, D. Beltran, A. B. Descalzo, G. Rodriguez-Lopez, R. Martinez-Manez, M. D. Marcos and P. Amoros, *Chem. Commun.*, 2002, 330.
13 A. Okabe, M. Niki, T. Fukushima and T. Aida, *J. Mater. Chem.*, 2005, **15**, 1329.
14 P. Yang, T. Deng, D. Zhao, P. Feng, D. Pine, B. F. Chmelka, G. M. Whitesides and G. D. Stucky, *Science*, 1998, **282**, 2244.
15 J. Pérez-Pariente, I. Díaz and J. Agúndez, *C. R. Chim.*, 2005, **8**, 569 and the references therein.
16 F. S. Xiao, *Catal. Surv. Asia*, 2004, **8**, 151 and the references therein.
17 L. Huang, Z. Wang, J. Sun, L. Miao, Q. Li, Y. Yan and D. Zhao, *J. Am. Chem. Soc.*, 2000, **122**, 3530.
18 (*a*) Y. J. Wang, Y. Tang, Z. Ni, W. M. Hua, W. L. Yang, X. D. Wang, W. C. Tao and Z. Gao, *Chem. Lett.*, 2000, 510; (*b*) A. A. Dong, Y. J. Wang, Y. Tang, Y. H. Zhang, N. Ren and Z. Gao, *Adv. Mater.*, 2002, **14**, 1506.
19 B. T. Holland, L. Abrams and A. Stein, *J. Am. Chem. Soc.*, 1999, **121**, 4308.
20 M. Antonietti, B. Berton, C. Göltner and H. Hentze, *Adv. Mater.*, 1998, **10**, 154.
21 B. Lebeau, C. E. Fowler, S. Mann, C. Farcet, B. Charleux and C. Sanchez, *J. Mater. Chem.*, 2000, **10**, 2105.
22 Q. Luo, L. Li, B. Yang and D. Zhao, *Chem. Lett.*, 2000, 378.
23 Z. Z. Yang, K. Qi, J. H. Rong, L. J. Wang, Z. P. Liu and Y. X. Yang, *Chin. Sci. Bull.*, 2001, **46**, 1785.
24 G. Gundiah, *Bull. Mater. Sci.*, 2001, **24**, 211.
25 S. Vaudreuil, M. Bousmina, S. Kaliaguine and L. Bonneviot, *Adv. Mater.*, 2001, **13**, 1310.
26 C. Danumah, S. Vaudreuil, L. Bonneviot, M. Bousmina, S. Giasson and S. Kaliaguine, *Microporous Mesoporous Mater.*, 2001, **44**, 241.
27 C. G. Oh, Y. Y. Baek and S. K. Ihm, *Adv. Mater.*, 2005, **17**, 270.
28 R. C. Schroden, C. F. Blanford, B. J. Melde, B. J. S. Johnson and A. Stein, *Chem. Mater.*, 2001, **13**, 1074.
29 (*a*) T. Sen, G. J. T. Tiddy, J. L. Casci and M. W. Anderson, *Angew. Chem., Int. Ed.*, 2003, **42**, 4649; (*b*) T. Sen, G. J. T. Tiddy, J. L. Casci and M. W. Anderson, *Chem. Mater.*, 2004, **16**, 2044.
30 K. R. Seddon, A. Stark and M. J. Torres, *Pure Appl. Chem.*, 2000, **72**, 2275.
31 (*a*) Y. Zhou and M. Antonietti, *Adv. Mater.*, 2003, **15**, 1452; (*b*) T. Brezesinski, C. Erpen, K. Iimura and B. Smarsly, *Chem. Mater.*, 2005, **17**, 1683; (*c*) Y. Zhou, J. H. Schattka and M. Antonietti, *Nano Lett.*, 2004, **4**, 477; (*d*) B. G. Trewyn, C. M. Whitman and V. S. Y. Lin, *Nano Lett.*, 2004, **4**, 2139.
32 Y. Zhou and M. Antonietti, *Chem. Commun.*, 2003, 2564.
33 D. B. Kuang, T. Brezesinski and B. Smarsly, *J. Am. Chem. Soc.*, 2004, **126**, 10534.
34 Y. Lu, H. Fan, N. Doke, D. A. Loy, R. A. Assink, D. A. Lavan and C. J. Brinker, *J. Am. Chem. Soc.*, 2000, **122**, 5258.
35 D. Grosso, G. J. A. A. Soler Illia, E. L. Crepaldi, B. Charleux and C. Sanchez, *Adv. Funct. Mater.*, 2003, **13**, 37.
36 (*a*) A. Imhof and D. J. Pine, *Nature*, 1997, **389**, 948; (*b*) A. Imhof and D. J. Pine, *Adv. Mater.*, 1998, **10**, 697.
37 (*a*) T. Sen, G. J. T. Tiddy, J. L. Casci and M. W. Anderson, *Microporous Mesoporous Mater.*, 2005, **78**, 255; (*b*) T. Sen, G. J. T. Tiddy, J. L. Casci and M. W. Anderson, *Chem. Commun.*, 2003, 2182.
38 H. F. Zhang, G. C. Hardy, M. J. Rosseinsky and A. I. Cooper, *Adv. Mater.*, 2003, **15**, 78.
39 F. Carn, A. Colin, M. F. Achard, H. Deleuze, E. Sellier, M. Birot and R. Backov, *J. Mater. Chem.*, 2004, **14**, 1370.
40 Z. Y. Yuan, T. Z. Ren and B. L. Su, *Adv. Mater.*, 2003, **15**, 1462.
41 H. G. Yang and H. C. Zeng, *Angew. Chem., Int. Ed.*, 2004, **43**, 5206.
42 D. M. Antonelli, *Microporous Mesoporous Mater.*, 1999, **33**, 209.
43 S. A. Bagshaw, *Chem. Commun.*, 1999, 767.
44 (*a*) F. Carn, A. Colin, M. F. Achard, H. Deleuze, Z. Saadi and R. Backov, *Adv. Mater.*, 2004, **16**, 140; (*b*) F. Carn, A. Colin,

M. F. Achard, H. Deleuze, C. Sanchez and R. Backov, *Adv. Mater.*, 2005, **17**, 62.
45 K. Suzuki, K. Ikari and H. Imai, *J. Mater. Chem.*, 2003, **13**, 1812.
46 R. A. Caruso and J. H. Schattka, *Adv. Mater.*, 2000, **12**, 1921.
47 R. A. Caruso and M. Antonietti, *Adv. Funct. Mater.*, 2002, **12**, 307.
48 P. R. Giunta, R. P. Washington, T. D. Campbell, O. Steinbock and A. E. Stiegman, *Angew. Chem., Int. Ed.*, 2004, **43**, 1505.
49 H. Maekawa, J. Esquena, S. Bishop, C. Solans and B. F. Chmelka, *Adv. Mater.*, 2003, **15**, 591.
50 (*a*) L. Huerta, C. Guillern, J. Latorre, A. Beltran, D. Beltran and P. Amoros, *Chem. Commun.*, 2003, 1448; (*b*) L. Huerta, C. Guillern, J. Latorre, A. Beltran, D. Beltran and P. Amoros, *Solid State Sci.*, 2005, **7**, 405.
51 S. A. Davis, S. L. Burkett, N. H. Mendelson and S. Mann, *Nature*, 1997, **385**, 420.
52 F. C. Meldrum and R. Seshadri, *Chem. Commun.*, 2000, 29.
53 D. Yang, L. Qi and J. Ma, *Adv. Mater.*, 2002, **14**, 1543.
54 G. Cook, P. L. Timms and C. Goeltner-Spickermann, *Angew. Chem., Int. Ed.*, 2003, **42**, 557.
55 S. R. Hall, H. Bolger and S. Mann, *Chem. Commun.*, 2003, 2784.
56 (*a*) V. Valtchev, M. Smaihi, A. C. Faust and L. Vidal, *Angew. Chem., Int. Ed.*, 2003, **42**, 2782; (*b*) V. Valtchev, M. Smaihi, A. C. Faust and L. Vidal, *Chem. Mater.*, 2003, **16**, 1350.
57 (*a*) Y. Shin, L. Q. Wang, J. H. Chang, W. D. Samuels and G. J. Exarhos, *Stud. Surf. Sci. Catal.*, 2003, **146**, 447; (*b*) L. Q. Wang, Y. Shin, W. D. Samuels, G. J. Exarhos, I. L. Moudrakovski, V. V. Terskikh and J. A. Ripmeester, *J. Phys. Chem. B*, 2003, **107**, 13793.
58 Y. Shin, C. Wang and G. J. Exarhos, *Adv. Mater.*, 2005, **17**, 73.
59 W. Ogasawara, W. Shenton, S. A. Davis and S. Mann, *Chem. Mater.*, 2000, **12**, 2835.
60 V. Pedroni, P. C. Schulz, M. E. G. de Ferreira and M. A. Morini, *Colloid Polym. Sci.*, 2000, **278**, 964.
61 B. Zhang, S. A. Davis and S. Mann, *Chem. Mater.*, 2002, **14**, 1369.
62 M. Iwasaki, S. A. Davis and S. Mann, *J. Sol-Gel Sci. Technol.*, 2004, **32**, 99.
63 D. Walsh, L. Arcelli, T. Ikoma, J. Tanaka and S. Mann, *Nat. Mater.*, 2003, **2**, 386.
64 D. Zhao, P. Yang, B. F. Chmelka and G. D. Stucky, *Chem. Mater.*, 1999, **11**, 1174.
65 H. Nishihara, S. R. Mukai, D. Yamashita and H. Tamon, *Chem. Mater.*, 2005, **17**, 683.
66 K. Nakanishi, *J. Porous Mater.*, 1997, **4**, 67.
67 (*a*) Y. Sato, K. Nakanishi, K. Hirao, H. Jinnai, M. Shibayama, Y. B. Melnichenko and G. D. Wignall, *Colloids Surf., A*, 2001, **187**, 117; (*b*) K. Nakanishi, Y. Sato, Y. Ruyat and K. Hirao, *J. Sol-Gel Sci. Technol.*, 2003, **26**, 567.
68 J. H. Smått, S. Schunk and M. Lindén, *Chem. Mater.*, 2003, **15**, 2354.
69 S. Murai, K. Fujita, K. Nakanishi and K. Hirao, *J. Phys. Chem. B*, 2004, **108**, 16670.
70 R. Takahashi, S. Sato, T. Sodesawa, K. Suzuki, M. Tafu, K. Nakanishi and N. Soga, *J. Am. Ceram. Soc.*, 2001, **84**, 1968.
71 J. Konishi, K. Fujita, K. Nakanishi and K. Hirao, *Mater. Res. Soc. Symp. Proc.*, 2004, **788**, L8.14.1.
72 K. Nakanishi, Y. Kobayashi, T. Amatani, K. Hirao and T. Kodaira, *Chem. Mater.*, 2004, **16**, 3652.
73 T. Amatani, K. Nakanishi, K. Hirao and T. Kodaira, *Chem. Mater.*, 2005, **17**, 2114.
74 Z. G. Shi, Y. Q. Feng, L. Xu, S. L. Da and Y. Y. Ren, *Microporous Mesoporous Mater.*, 2004, **68**, 55.
75 (*a*) N. Huesing, C. Raab, V. Torma, A. Roig and H. Peterlik, *Chem. Mater.*, 2003, **15**, 2690; (*b*) N. Huesing, C. Raab and V. Torma, *Mater. Res. Soc. Symp. Proc.*, 2003, **775**, 9.
76 D. Brandhuber, V. Torma, C. Raab, H. Peterlik, A. Kulak and N. Huesing, *Chem. Mater.*, 2005, **17**, 4262.
77 B. L. Su, A. Léonard and Z. Y. Yuan, *C. R. Chim.*, 2005, **8**, 713.
78 J. L. Blin, A. Leonard, Z. Y. Yuan, L. Gigot, A. Vantomme, A. K. Cheetham and B. L. Su, *Angew. Chem., Int. Ed.*, 2003, **42**, 2872.
79 Z. Y. Yuan, A. Vantomme, A. Léonard and B. L. Su, *Chem. Commun.*, 2003, 1558.
80 W. Deng, M. W. Toepke and B. H. Shanks, *Adv. Funct. Mater.*, 2003, **13**, 61.
81 T. Z. Ren, Z. Y. Yuan and B. L. Su, *Langmuir*, 2004, **20**, 1531.
82 A. Leonard, J. L. Blin and B. L. Su, *Chem. Commun.*, 2003, 2568.
83 Z. Y. Yuan, T. Z. Ren, A. Vantomme and B. L. Su, *Chem. Mater.*, 2004, **16**, 5096.
84 A. Collins, D. Carriazo, S. A. Davis and S. Mann, *Chem. Commun.*, 2004, 568.
85 A. Leonard and B. L. Su, *Chem. Commun.*, 2004, 1674.
86 W. H. Deng and B. H. Shanks, *Chem. Mater.*, 2005, **17**, 3092.
87 T. Z. Ren, Z. Y. Yuan and B. L. Su, *Chem. Commun.*, 2004, 2730.
88 Z. Y. Yuan, T. Z. Ren, A. Azioune, J. J. Pireaux and B. L. Su, *Chem. Mater.*, 2005, submitted.
89 T. Z. Ren, Z. Y. Yuan and B. L. Su, *Chem. Phys. Lett.*, 2004, **388**, 46.
90 A. Corma, *Chem. Rev.*, 1997, **97**, 2373.
91 T. Z. Ren, Z. Y. Yuan, A. Azioune and B. L. Su, *Langmuir*, 2005, submitted.
92 H. Chen, J. Gu, J. Shi, Z. Liu, J. Gao, M. Ruan and D. Yan, *Adv. Mater.*, 2005, **17**, 2010.
93 H. Yang and D. Zhao, *J. Mater. Chem.*, 2005, **15**, 1217.
94 A. Taguchi, J. H. Smatt and M. Lindén, *Adv. Mater.*, 2003, **15**, 1209.
95 A. H. Lu, J. H. Smatt, S. Backlund and M. Lindén, *Microporous Mesoporous Mater.*, 2004, **72**, 59.
96 Z. G. Shi, Y. Q. Feng, L. Xu, S. L. Da and M. Zhang, *Carbon*, 2003, **41**, 2677.
97 G. S. Chai, I. S. Shin and J. S. Yu, *Adv. Mater.*, 2004, **16**, 2057.
98 N. Tanaka, H. Kobayashi, K. Nakanishi, H. Minakuchi and N. Ishizuka, *Anal. Chem.*, 2001, **73**, 420A.
99 N. Ishizuka, H. Minakuchi, K. Nakanishi, N. Soga and N. Tanaka, *J. Chromatogr., A*, 1998, **797**, 133.
100 N. Ishizuka, H. Minakuchi, K. Nakanishi, K. Hirao and N. Tanaka, *Colloids Surf., A*, 2001, **187**, 273.
101 E. Prouzet and C. Boissière, *C. R. Chim.*, 2005, **8**, 579.
102 R. Takahashi, S. Sato, T. Sodesawa and M. Yabuki, *J. Catal.*, 2001, **200**, 197.
103 N. Nakamura, R. Takahashi, S. Sato, T. Sodesawa and S. Yoshida, *Phys. Chem. Chem. Phys.*, 2000, **2**, 4983.
104 J. J. Chiu, D. J. Pine, S. T. Bishop and B. F. Chmelka, *J. Catal.*, 2004, **221**, 400.
105 X. Wang, J. C. Yu, C. Ho, Y. Hou and X. Fu, *Langmuir*, 2005, **21**, 2552.
106 Z. Y. Yuan, T. Z. Ren, A. Azioune, J. J. Pireaux and B. L. Su, *Catal. Today*, 2005, **105**, 647.
107 H. L. Tidahy, S. Siffert, J.-F. Lamonier, E. A. Zhilinskaya, A. Aboukaïs, Z. Y. Yuan, A. Vantomme, B.-L. Su, X. Canet, G. Deweireld and M. Frère, *Stud. Surf. Sci. Catal.*, 2005, in press.
108 C. Ho, J. C. Yu, X. Wang, S. Lai and Y. Qiu, *J. Mater. Chem.*, 2005, **15**, 2193.
109 (*a*) M. Mamak, N. Coombs and G. A. Ozin, *J. Am. Chem. Soc.*, 2000, **122**, 8932; (*b*) M. Mamak, N. Coombs and G. A. Ozin, *Adv. Funct. Mater.*, 2001, **11**, 59.
110 A. Vantome, Z. Y. Yuan and B. L. Su, unpublished.
111 J. S. Yu, S. Kang, S. B. Yoon and G. Chai, *J. Am. Chem. Soc.*, 2002, **124**, 9382.
112 K. Unger, H. Rupprecht, B. Valentin and W. Kircher, *Drug Dev. Ind. Pharm.*, 1983, **9**, 69.
113 J. Andersson, J. Rosenholm, S. Areva and M. Lindén, *Chem. Mater.*, 2004, **16**, 4160.
114 J. Lee, J. Kim, J. Kim, H. Jia, M. I. Kim, J. H. Kwak, S. Jin, A. Dohnalkova, H. G. Park, H. N. Chang, P. Wang, J. W. Grate and T. Hyeon, *Small*, 2005, **1**, 744.
115 M. Tortajada, D. Ramón, D. Beltrán and P. Amorós, *J. Mater. Chem.*, 2005, **15**, 3859.
116 M. Kitamura, C. Ohtsuki, S. Ogata, M. Kamitakahara and M. Tanihara, *Mater. Trans.*, 2004, **45**, 983.
117 M. Kitamura, C. Ohtsuki, S. Ogata, M. Kamitakahara and M. Tanihara, *J. Am. Ceram. Soc.*, 2005, **88**, 822.
118 V. V. Guliants, M. A. Carreon and Y. S. Lin, *J. Membr. Sci.*, 2004, **235**, 53.
119 S. Mann, *Chem. Commun.*, 2004, 1.
120 J. Aizenberg, J. C. Weaver, M. S. Thanawala, V. C. Sunder, D. E. Morse and P. Fratzl, *Science*, 2005, **309**, 275.
121 Y. Shimizu, T. Hyodo and M. Egashira, *Catal. Surv. Asia*, 2004, **8**, 127 and the references therein.
122 C. J. Martinez, B. Hockey, C. B. Montgomery and S. Semancik, *Langmuir*, 2005, **21**, 7937.